

FIG. 4. Normalized strain as a function of applied electric field which clearly shows the existence of a threshold field.

does not cause a remnant effect which clearly indicates that a threshold field required for polarization reversal exists. This threshold effect is more clearly illustrated in Fig. 4. This figure is a plot of normalized (computed from Bragg's law) strain versus electric field and shows a threshold field required for polarization reversal of approximately 3 kV/cm. This agrees well with threshold switching field values obtained by Pulvari⁴ from electric measurements.

CONCLUSIONS

The existence of a distinct threshold field required for polarization reversal is one of the most important

properties of ferrielectric materials and was never observed in ordinary ferroelectrics. Before this investigation the only means of detecting a threshold field was through direct electrical methods. The ability to detect a threshold with x-ray techniques provides an additional method. More important, the change in Bragg diffraction conditions shows that a small, but distinct, physical crystallographic structure rearrangement occurs as a ferrielectric material is switched from one polarization state to another. Although it was previously known that small relative shifts of atomic positions do occur, it was not known that remnant structure rearrangements of the unit cell occur. Even though the detailed process of the switching mechanism which produces this effect is not presently completely understood, it appears that the origin of the threshold field required for polarization reversal can be traced to minute remnant rearrangements of the structure.

ACKNOWLEDGMENT

I wish to express my sincere gratitude to Professor Charles F. Pulvari for suggesting this topic and for his guidance and discussions during the work.

Theory of Thermionic Converter Extinguished-Mode Operation with Applications to Converter Diagnostics*

DANIEL R. WILKINS† AND ELIAS P. GYFTOPOULOS

*Department of Nuclear Engineering and Research Laboratory of Electronics,
Massachusetts Institute of Technology, Cambridge, Massachusetts*

(Received 11 April 1966; in final form 24 June 1966)

An analysis of thermoionic converters operating in the extinguished mode is presented. Expressions for the forward and reverse saturation output current densities, and for the open circuit voltage are derived for the first time from a single set of transport equations and boundary conditions. Agreement between theoretical and experimental results is established. It is shown that the output current density cannot exceed a certain upper limit which depends only upon the emitter temperature and the interelectrode spacing, and is independent of the emitter work function and the cesium pressure. It is shown that, under certain operating conditions, measurements of the forward and reverse saturation output-current densities and of the open circuit voltage can be used to infer values of the emitter temperature, emitter work function, collector work function, and electron and ion mobilities.

1. INTRODUCTION

THE purposes of this paper are to present a unified analysis of the extinguished mode of cesium thermionic-converter operation, and to demonstrate the utility of extinguished mode measurements in converter diagnostics.

* This work was supported in part by the Joint Services Electronic Program (Contract DA36-039-AMC-03200(E)) and the National Science Foundation (Grant GK-1165).

† Present address: General Electric Company, Special Purpose Nuclear Systems Operation, Pleasanton, Calif.

The output-current characteristics of a thermionic converter frequently exhibit two distinct branches as shown schematically in Fig. 1. The upper branch is referred to herein as the "ignited mode" of operation; the lower branch as the "extinguished mode." For a wide variety of operating conditions, the lower branch exhibits forward and reverse saturation current densities and an open circuit voltage as indicated in Fig. 1. It is toward the analysis of this extinguished mode output-current characteristic that the present study is directed.

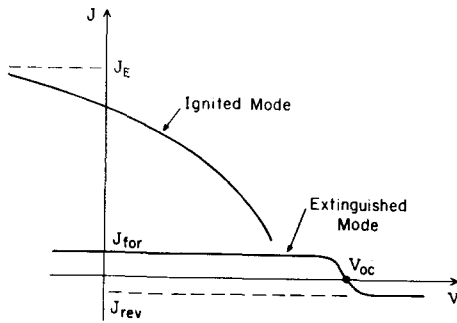


FIG. 1. Schematic of output-current characteristic of a thermionic converter operating in the collisional regime.

Several features of the extinguished mode have been analyzed in previous studies.¹⁻⁷ Shavit and Hatsopoulos,¹ Warner and Hansen,²⁻⁴ and Warner⁵ derived expressions for the "forward saturation current density J_{for} " (see Fig. 1). Wilkins⁶ derived an expression for the open circuit voltage V_{oc} . Houston⁷ presented an expression for the "reverse saturation current density J_{rev} " (see Fig. 1) which is applicable in the limit of negligible collector back emission.

In this paper, the forward and reverse saturation current densities, and the open-circuit voltage are derived for the first time from a single set of transport equations and boundary conditions. In addition, the implications of these results in thermionic-converter diagnostics are emphasized. The transport equations are the same as those derived in Ref. 8 and used to analyze thermionic converters operating in the ignited mode.⁹ Thus, a single unified description of the entire collisional regime of thermionic-converter operation is achieved.

The paper is divided into four parts. First, the plasma transport differential equation⁸ are presented in a form suitable for extinguished mode analyses. The boundary conditions which must be satisfied by the solutions of these equations are also given. Second, expressions for the forward saturation current density are derived and interpreted for use in converter diagnostics. Third, expressions for the reverse saturation current density and open-circuit voltage are derived and their use in converter diagnostics is discussed. Fourth, the results of

the above investigations are compared with experimental data and agreement between theory and experiment is established.

The methods and equations of this paper can also be used to derive complete output-current characteristics of thermionic converters operating in the extinguished mode. Such characteristics, however, are not included herein.

2. TRANSPORT EQUATIONS AND BOUNDARY CONDITIONS

2.1. Transport Equations

Cesium plasmas in thermionic converters operating in the extinguished mode have several characteristic properties which, when reflected in the plasma transport differential equations of Ref. 8, lead to mathematical simplifications. First, the electron and ion densities, n_e and n_i , respectively, are sufficiently low that charged-particle interactions may be neglected. Second, inelastic collisions are negligible because of the low electron densities and temperatures involved. Third, since the net electron current is small compared to the random electron current throughout most of the plasma, the plasma electron temperature may be assumed constant and equal to the emitter temperature. Thus, if the heavy-particle temperature gradients are neglected and the interelectrode plasma is assumed neutral, the transport equations reduce to a set of two equations of the form:

$$J_i = -\mu_i^0 [kT_i (dn/dx) - enE], \quad (1)$$

$$J_e = J_i + J = -\mu_e^0 [kT_e (dn/dx) + enE], \quad \text{for } T_e = T_E, \quad (2)$$

where J_α and T_α ($\alpha = e, i$) are the uniform current density and temperature of species α , respectively; n is the charged particle density; μ_α^0 is the mobility of species α in the absence of charged-particle collisions;⁸ J is the output current density; and E is the electric field of the plasma.

2.2. Boundary Conditions

The solutions of Eqs. (1)-(2) involve integration constants which may be evaluated through the use of boundary conditions. These boundary conditions are obtained by writing electron and ion current balances across the Debye sheaths at the plasma-electrode interfaces. The exact form of a particular balance depends upon the polarity of the sheath. For convenience, a sheath polarity is called accelerating or retarding if the sheath accelerates or retards an electron traveling in the direction from the emitter to the collector, respectively.

Boundary conditions for accelerating and retarding emitter and collector sheaths are given in Table I. In this table, V_{ES} and V_{CS} are the emitter and collector sheath voltage drops, respectively; T_E and T_C are the emitter and collector temperatures, respectively; J_r

¹ A. Shavit and G. N. Hatsopoulos, *Proceedings of the Thermionic Conversion Specialist Conference, Cleveland, Ohio*, October 1964, pp. 206-213.

² L. K. Hansen and C. Warner, Ref. 1, pp. 310-315.

³ C. Warner and L. K. Hansen, 23rd Annual Phys. Elec. Conference, M. I. T., Cambridge, Mass., March 1963, pp. 400-405.

⁴ L. K. Hansen and C. Warner, *Proceedings of the Thermionic Conversion Specialist Conference, Gallinburg, Tenn.*, October 1963, pp. 44-50.

⁵ C. Warner, Ref. 4, pp. 51-56.

⁶ D. R. Wilkins, Ref. 1, pp. 275-283.

⁷ J. M. Houston, Proc. 24th Annual Conference on Phys. Elec., M. I. T., Cambridge, Mass. (March 1964), pp. 211-223.

⁸ D. R. Wilkins and E. P. Gyftopoulos, *J. Appl. Phys.* **37**, 3533 (1966).

⁹ D. R. Wilkins and E. P. Gyftopoulos, *J. Appl. Phys.* **37**, 2892 (1966).

TABLE I. Boundary conditions for the plasma transport equations.

Accelerating emitter sheath	Retarding emitter sheath
$J_e = J_E - J_r(0) \exp(-eV_{ES}/kT_E)$	$J_e = J_E \exp(-eV_{ES}/kT_E) - J_r(0)$
$J_i = I_E \exp(-eV_{ES}/kT_E) - I_r(0)$	$J_i = I_E - I_r(0) \exp(-eV_{ES}/kT_E)$
Accelerating collector sheath	Retarding collector sheath
$J_e = J_r(d) - J_C \exp(-eV_{CS}/kT_C)$	$J_e = J_r(d) \exp(-eV_{CS}/kT_E) - J_C$
$J_i = I_r(d) \exp(-eV_{CS}/kT_i)$	$J_i = I_r(d)$

and I_r are the plasma electron and ion random current densities, respectively; J_E and I_E are the electron and ion emission current densities from the emitter, respectively; J_C is the collector back emission; the notations $H(0)$ and $H(d)$ are used to denote any x -dependent quantity $H(x)$ evaluated at the emitter edge ($x=0$) and at the collector edge ($x=d$) of the plasma, respectively; and surface ionization at the collector is neglected. The boundary conditions are not exact since they do not account for the non-Maxwellian, anisotropic nature of the charged-particle distribution functions in the interelectrode space. Although first-order corrections which account for these effects can be included, the resulting relations are not sufficiently different to justify the added complexity. It should also be noted that no electron kinetic energy flux balances are included in Table I. This is consistent with the constancy of the electron temperature.

The electron emission current densities from the emitter and collector are given by the relations:

$$J_E = AT_E^2 \exp(-e\phi_E/kT_E)$$

$$J_C = AT_C^2 \exp(-e\phi_C/kT_C), \quad (3)$$

and

where $A=120(\text{A}/\text{cm}^2 \cdot \text{K}^2)$, and ϕ_E and ϕ_C are the emitter and collector work functions, respectively.

The ion-emission current density from the emitter is given by the approximate Saha-Langmuir equation:

$$I_E = e p_{Cs} (2\pi m_i k T_E)^{-\frac{1}{2}} \exp[-e(V_i - \phi_E)/kT_E], \quad (4)$$

where p_{Cs} , m_i , and V_i are the pressure, mass, and ionization potential of cesium, respectively. The approximation is valid for $e(V_i - \phi_E) \gg kT_E$, which is generally true for thermionic converters.

2.3. Extinguished Mode Analyses

Equations (1) and (2) and the boundary conditions of Table I provide the basis for the analysis of the extinguished mode. Such analyses proceed as follows: (a) sheath polarities are specified; (b) the charged-particle density and electric field profiles, and the sheath voltage drops are determined from Eqs. (1) and (2) and the corresponding boundary conditions; (c) the output current vs output voltage relation is computed; and (d) the operating conditions for which the specified sheath polarities prevail is established, i.e., the region of validity of step (a) is defined. For operating

conditions outside this region of validity alternate sheath polarities are considered.

In Secs. 3 and 4 the above procedure is used to derive expressions for several characteristic quantities associated with extinguished mode output-current characteristics, namely J_{for} , J_{rev} , and V_{oc} .

3. FORWARD SATURATION CURRENT DENSITY

At low output voltages, an extinguished mode output-current characteristic saturates at a forward saturation current density J_{for} as shown in Fig. 1. An expression for this limiting output-current density is derived below.

When the output voltage $V \ll 0$, the collector sheath becomes accelerating, $J_i \rightarrow 0$, and $J_e = J = J_{\text{for}}$. Thus, Eqs. (1) and (2) and the boundary conditions (Table I) for an accelerating collector sheath yield

$$J_r(x) = J_{\text{for}}[1 + R_e'(1-x/d)];$$

$$R_e' \equiv e\bar{v}_e d / 4\mu_0^0 k(T_E + T_i), \quad (5)$$

where \bar{v}_e is the average thermal speed of particles of species α . Note that R_e' is closely related to the interelectrode spacing measured in electron-neutral mean-free paths. For hard-sphere collisions,

$$R_e' = \frac{3}{4} [T_E / (T_E + T_i)] n_0 \sigma_{e0} d,$$

where n_0 is the neutral cesium density and σ_{e0} is the electron-neutral cross section.

Equation (5) must be combined with the boundary conditions at the emitter edge of the plasma to yield an expression for J_{for} . Two possibilities exist since the emitter sheath may be either accelerating or retarding.

3.1. J_{for} for Accelerating Emitter Sheaths

For accelerating emitter sheaths, Eq. (5) and the boundary conditions of Table I yield an expression for J_{for} which may be written in two convenient forms, namely:

$$J_{\text{for}}/J_E = 2\theta[(1+\theta^2)^{\frac{1}{2}} - \theta], \quad \theta \equiv \beta^{\frac{1}{2}} / 2(1+R_e'); \quad (6a)$$

$$J_{\text{for}} = [J_r^* / (1+R_e')] [(1+\theta^2)^{\frac{1}{2}} - \theta]; \quad (6b)$$

where β is the ion-richness ratio given by the relation

$$\beta = (m_i/m_e)^{\frac{1}{2}} I_E/J_E, \quad (7)$$

$J_r^* = en^* \bar{v}_e / 4$, and n^* is the charged-particle density in a neutral plasma in thermodynamic equilibrium with the emitter and is given by the relation

$$n^* = (p_{Cs}/kT_E)^{\frac{1}{2}} (2\pi m_e k T_E / h^2)^{\frac{3}{2}} \exp(-eV_i/2kT_E). \quad (8)$$

Equations (6) are valid, i.e., the emitter sheath is accelerating, provided the ion-richness β is greater than a critical value β_{cr} given by the relation

$$\beta_{cr} \equiv (1+R_e') / (2+R_e'). \quad (9)$$

The meaning of Eq. (6a) is that the ratio J_{for}/J_E

depends only upon the ion-richness ratio β and the number of electron-neutral mean-free paths R_e' across the plasma. This conclusion has been reached independently by Shavit and Hatsopoulos¹ and Hansen and Warner.² The form of Eq. (6a), however, is different from that derived by the previous authors due to different approximations regarding the plasma electron distribution function.

For $\theta \gg 1$, Eq. (6a) takes the simpler form

$$J_{\text{for}} \approx J_E, \text{ for } \theta \gg 1. \quad (6c)$$

In other words, under this condition the forward saturation current density is electron-emission-limited and depends strongly upon the emitter work function. On the other hand, for $\theta \ll 1$, Eq. (6b) becomes

$$J_{\text{for}} \approx J_r^*/(1+R_e'), \text{ for } \theta \ll 1. \quad (6d)$$

This implies that J_{for} is determined by the plasma properties and is independent of the emitter work function.

Equations (6c) and (6d), for $\beta \geq \beta_{cr}$, are useful in converter diagnostics. For example, when Eq. (6c) is applicable and T_E is known, a measurement of J_{for} yields J_E and hence the emitter work function. When Eq. (6d) is applicable and R_e' is known, then a measurement of J_{for} yields J_r^* . Since J_r^* is extremely sensitive to the emitter temperature, this measurement provides a means of accurately determining T_E in devices in which the emitter is not accessible for temperature measurements. Also, when Eq. (6d) is applicable, a plot of experimental data on $1/J_{\text{for}}$ vs d should yield a straight line. If p_{Cs} is known, the intercept of this line at $d=0$ yields $1/J_r^*$, while the slope yields the electron mobility.

3.2. J_{for} for Retarding Emitter Sheaths

For retarding emitter sheaths the combination of Eq. (5) with the corresponding boundary conditions yield J_{for} for $\beta \leq \beta_{cr}$. The results may again be written in two convenient forms, namely:

$$J_{\text{for}}/J_E = [\beta^{1/2}/(1+R_e')][(1+R_e')/(2+R_e')]^{1/2}, \quad (10a)$$

$$J_{\text{for}} = [J_r^*/(1+R_e')][(1+R_e')/(2+R_e')]^{1/2} \\ = \beta_{cr}^{1/2} J_r^*/(1+R_e'). \quad (10b)$$

The meaning of these equations is that the forward saturation current density for $\beta \leq \beta_{cr}$ is determined by ion emission and plasma effects rather than by electron emission and plasma effects. The relative importance of these effects is brought forth by Eq. (10a). For $R_e' \gg 1$, the factor $\beta^{1/2}$ is the probability that an electron surmounts the emitter sheath barrier which arises from insufficient ion emission, and the factor $1/(1+R_e')$ is the probability that an electron diffuses through the plasma to the collector. Equation (10a) has been reported previously by Warner and Hansen.³

Note also that Eq. (10b) for $\beta \leq \beta_{cr}$ may be used in converter diagnostics in the same manner as discussed previously in connection with Eq. (6d) for $\beta \geq \beta_{cr}$.

3.3. Implication of the J_{for} Results

The forward saturation current density is the largest current density which can be achieved under conditions of extinguished mode operation. The upper limit of this density is given by Eq. (10b). This upper limit depends only upon p_{Cs} , T_E , and d and is independent of the emitter work function. Furthermore, for given practical emitter temperature and interelectrode spacing, there is an optimum cesium pressure at which the upper limit of J_{for} is a maximum. This maximum cannot be exceeded regardless of the choice of emitter work function or cesium pressure or both. Consequently, the surface ionization scheme for electron space-charge neutralization is limited.

4. REVERSE SATURATION CURRENT—OPEN CIRCUIT VOLTAGE

4.1. Output Current Characteristics

The reverse saturation current J_{rev} and the open circuit voltage V_{oc} can be found from the output-current characteristics for output voltages in the vicinity of V_{oc} and higher. For such output voltages, the currents through the converter satisfy the inequality

$$J_e/J_i \ll \mu_e^0/\mu_i^0, \quad (11)$$

and the collector sheath is, in general, retarding. Under these conditions, integration of Eqs. (1) and (2) yields

$$I_r(x) = J_i[1+R_i'(1-x/d)], \quad (12)$$

$$R_i' \equiv e\bar{v}_i d/4\mu_i^0 k(T_E+T_i);$$

$$V_p = (kT_E/e) \ln(1+R_i'); \quad (13)$$

$$V_{CS} = (kT_E/e) \ln[(m_i/m_e)^{1/2} J_i/(J_e+J_C)]; \quad (14)$$

where R_i' is a quantity analogous to R_e' [Eq. (5)] and is closely related to the interelectrode spacing measured in terms of ion-neutral mean-free paths, and V_p is the plasma voltage drop. Note that in the absence of collector back emission ($J_C=0$) the collector sheath is retarding provided $J_e/J_i < (m_i/m_e)^{1/2}$. This condition is always satisfied in the range of output voltages under consideration.

The output-current characteristics are derived by combining Eqs. (12)–(14) with the emitter sheath boundary conditions. Provided $J_e \ll J_E$, these characteristics, for either accelerating or retarding emitter sheaths, are given by the relation:

$$J = J_r^* \exp[-e(V+\phi_C-\phi_p^*)/kT_E] - (J_i+J_C), \quad (15)$$

where V is the output voltage, and ϕ_p^* is the chemical potential, measured relative to the Fermi level of the emitter,⁴ of a neutral plasma in thermodynamic equilib-

rium with the emitter. This potential is given by the relation

$$\phi_p^* = V_i/2 + (kT_E/2e) \ln[4(2\pi m_e/h^2)^{3/2}(kT_E)^{3/2}p_{Cs}]. \quad (16)$$

Although Eq. (16) is valid regardless of the emitter sheath polarity, the ion current J_i depends on that polarity.

J_i for Accelerating Emitter Sheaths

For accelerating emitter sheaths, Eq. (12) and the boundary conditions (Table I) yield that the ion current is given by the relation

$$J_i = [I_r^*/(1+R_i')] [(1+R_i')/(2+R_i')]^{1/2}, \quad (17)$$

where $I_r^* = en^*\hat{v}_i/4$. Equation (17) is valid, namely the emitter sheath is accelerating, provided the ion richness ratio β is greater than a critical value β_{cr}' given by the relation

$$\beta_{cr}' = (2+R_i')/(1+R_i'). \quad (18)$$

Equation (17) has been derived previously by Houston.⁷

J_i for Retarding Emitter Sheaths

For retarding emitter sheaths, namely $\beta \leq \beta_{cr}$, J_i is given by the relation

$$J_i = [I_r^*/(1+R_i')] [(1+\eta^2)^{1/2} - \eta]; \quad (19)$$

$$\eta \approx \frac{1}{2}(1+R_i')\beta^{1/2}.$$

Two limiting forms of Eq. (19) are of particular interest, namely;

$$J_i \approx I_E, \quad \text{for } \eta \gg 1; \quad (19a)$$

$$J_i \approx I_r^*/(1+R_i'), \quad \text{for } \eta \ll 1. \quad (19b)$$

4.2. Reverse Saturation Current Density

The reverse saturation current density J_{rev} is derived from Eq. (15) for $V \gg 0$. Thus,

$$J_{rev} = J_i + J_C, \quad (20)$$

where J_i is given either by Eq. (17) for $\beta \geq \beta_{cr}'$ or by Eq. (19) for $\beta \leq \beta_{cr}'$.

For $J_C \ll J_i$, the reverse saturation current density is given directly by Eq. (17) or (19). The formal similarity of Eqs. (17) and (19) to Eqs. (10b) and (6b), respectively, reflects the fact that, for $J_C \ll J_i$, the forward and reverse saturation current densities merely correspond to different particle species reaching the collector. Because of this similarity, Eqs. (17) and (19) are useful in converter diagnostics in the same manner as Eqs. (10b) and (6b), respectively. In particular, if $J_C \ll J_i$, measurements of J_{rev} can be used to infer values of T_E , ϕ_E , and μ_i^0 .

In general, if J_i is known, either from measurements at very low T_C or from theory, Eq. (20) permits a determination of J_C from a measurement of J_{rev} . Thus, the collector work function ϕ_C follows if T_C is known.

4.3. Open Circuit Voltage

The open-circuit voltage V_{oc} follows directly from Eq. (15) for $J=0$. Thus,

$$V_{oc} = \phi_p^* + (kT_E/e) \ln[J_r^*/J_{rev}] - \phi_C. \quad (21)$$

This result is only slightly different from that reported in Ref. 6.

The open-circuit voltage is particularly useful in converter diagnostics when coupled with measurements of J_{rev} . Specifically if T_E and p_{Cs} (and hence ϕ_p^* and J_r^*) are known, measurements of V_{oc} and J_{rev} yield the collector work function.

5. COMPARISON OF THEORY AND EXPERIMENT

5.1. Comparison of Theoretical and Experimental J_{for} Results

Warner and Hansen⁸ have reported experimental data on J_{for} for the case of $\beta < \beta_{cr} = 1$. By plotting their results, for fixed T_E , on a $1/J_{for}$ vs d plot, and utilizing a theoretical expression similar to Eq. (10a), they were able to infer a value for the electron-neutral cross section of $\sigma_{eo} \approx 200 \text{ \AA}^2$. Because of uncertainties in their estimate of the emitter work function, the value inferred for σ_{eo} was considered approximate.

Although the procedure employed by Warner and Hansen is correct, it does not recognize an important feature of the theoretical expression for J_{for} for $\beta < \beta_{cr}$; namely that J_{for} is independent of the emitter work function. This independence is brought forth by Eq. (10b), and permits a determination of σ_{eo} which is not subject to errors in the estimated emitter work function.

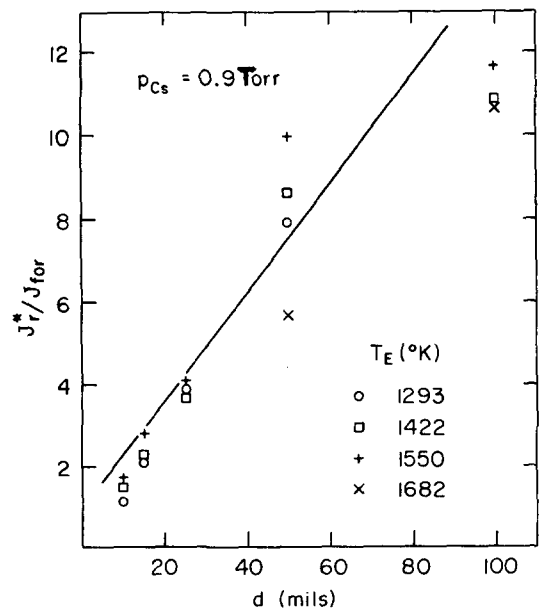


FIG. 2. Comparison of theoretical J_r^*/J_{for} vs d [solid line—Eq. (10b)] with experimental data from Ref. 3.

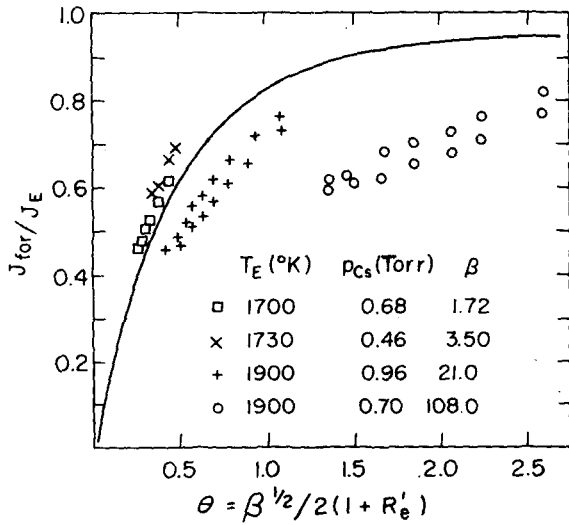


FIG. 3. Plot of theoretical J_{for}/J_E vs θ [solid line—Eq. (6a)]. Superimposed also are experimental data reported in Ref. 1. The theory is not strictly applicable to these data.

Figure 2 shows the Warner-Hansen data³ on a J_r^*/J_{for} plot as suggested by Eq. (10b). The data for the several emitter temperatures indeed fall reasonably close to a single straight line when plotted in this manner. From the slope of this line a value of $\sigma_{eo} = 180 \pm 100 \text{ \AA}^2$ is inferred if the average background gas temperature is assumed to be 1200°K. This value confirms the Warner-Hansen estimate.³ The present value ($\sigma_{eo} = 180 \pm 100 \text{ \AA}^2$) should also be compared with: (a) the values $\sigma_{eo} \approx 40\text{--}1000 \text{ \AA}^2$ obtained from various theoretical and experimental studies and tabulated by Houston¹⁰; (b) the value $\sigma_{eo} = 400 \text{ \AA}^2$ suggested by Houston¹⁰ as an appropriate average of existing data; and (c) the values $\sigma_{eo} \approx 260\text{--}1500 \text{ \AA}^2$ inferred from ignited-mode measurements.⁹

The theoretical J_{for}/J_E vs d relation for $\beta \geq \beta_{cr}$ [Eq. (6a)] is shown in Fig. 3. No appropriate experimental data for truly collision dominated operation is available for comparison with this result. Shavit and Hatsopoulos,¹ however, have reported experimental data on approximate values of J_{for} for $\beta \geq \beta_{cr}$ and $R_e' \leq 5$. For lack of more appropriate measurements these data are plotted in Fig. 3 assuming that $\sigma_{eo} = 400 \text{ \AA}^2$. The agreement between theory and experiment for $\beta = 1.72, 3.5, \text{ and } 21$ is surprisingly good considering the small number of mean-free paths across the plasma, and the fact that the data do not represent truly J_{for} . The agreement for $\beta = 108$ is less favorable.

5.2. Comparison of Theoretical and Experimental J_{rev} Results

Houston⁷ has reported experimental data for J_{rev} obtained under operating conditions for which the emission is ion-rich ($\beta > \beta_{cr} \approx 1$) and back emission from the

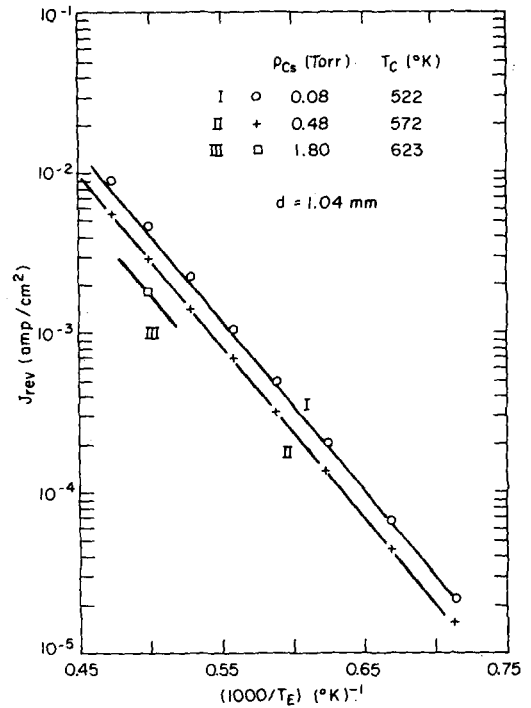


FIG. 4. Comparison of theoretical J_{rev} vs $1/T_E$ [solid lines—Eq. (17)] with experimental data from Ref. 5.

collector is negligible. He compared his results with Eq. (17) and found that the best agreement between theory and experiment was obtained using the ion mobility $\mu_i^0 = 0.32 \times 10^{19}/n_0 \text{ cm}^2/\text{V}\cdot\text{sec}$. Based on this value of the ion mobility, Houston's comparison of theory and experiment is shown in Fig. 4. In this figure, the solid curves are the theoretical predictions of Eq. (17) and the datum points are experimental. The agreement is indeed excellent over a 800°K range in emitter temperature and for an order of magnitude variation in cesium pressure. Houston⁷ has compared the inferred value for μ_i^0 with independent measurements and found satisfactory agreement.

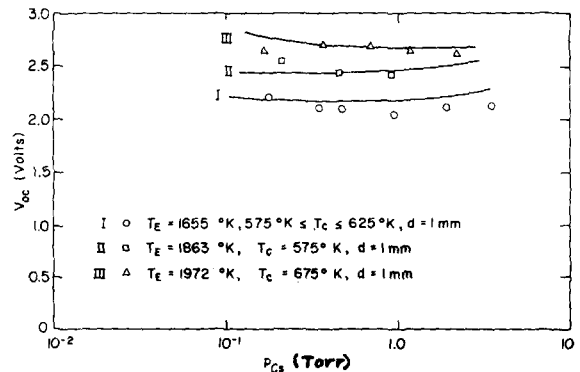


FIG. 5. Comparison of theoretical V_{oc} vs p_{Cs} [solid lines—Eqs. (21) and (17)] with experimental data from Ref. 9.

¹⁰ J. M. Houston, Ref. 1, pp. 300-309.

5.3. Comparison of Theoretical and Experimental V_{oc} Results

Figure 5 shows plots of open-circuit voltage vs cesium pressure for several emitter temperatures. The data were obtained by Reichelt¹¹ and correspond to operating conditions for which the emission is ion-rich and the collector back emission is negligible. The solid curves are the theoretical predictions of Eqs. (21) and (17) for the same ion mobility as above. Collector work functions for the cesium-covered nickel collector are determined by scaling the work-function data of Rump *et al.*¹² into the cesium pressure region of interest, as described in Ref. 6. The theoretical curves are bounded on the left at the cesium pressure for which $R_i' = 1.0$. The agreement between theoretical and experimental results

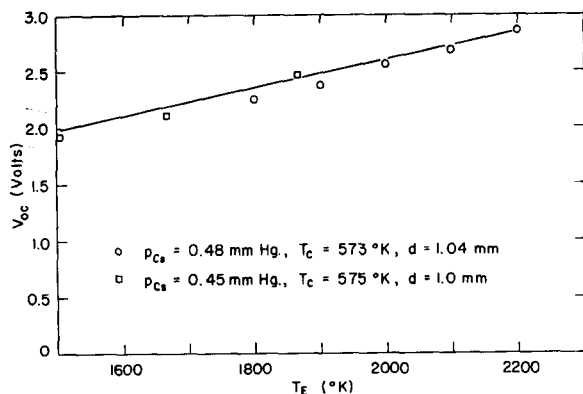


FIG. 6. Comparison of the theoretical V_{oc} vs T_E [solid line—Eqs. (21) and (17)] with experimental data from Refs. 9 and 5.

¹¹ W. Reichelt, Los Alamos Scientific Laboratory (private communication August 1964).

¹² B. S. Rump, J. F. Bryant, and B. L. Gehman, Ref. 3, pp. 232–238.

is good. Maximum discrepancies are approximately equal to five percent.

Figure 6 shows a plot of open-circuit voltage vs emitter temperature for $p_{Cs} \approx 0.45$ Torr. The low-temperature data were obtained by Reichelt¹¹ and the high-temperature data by Houston.⁷ In each case the emission was ion-rich, the collector temperature was sufficiently low that back emission was negligible, and $\phi_c \approx 1.81$ eV. The solid line in Fig. 6 is the theoretical prediction of Eqs. (21) and (17). The agreement of the theoretical curve with both sets of data is excellent. Errors are less than several percent over a 700°K range in emitter temperature.

6. CONCLUSIONS

Theoretical expressions for the forward and reverse saturation current densities and open-circuit voltage of cesium thermionic converters operating in the collisional extinguished mode are derived for the first time from a single set of transport equations and boundary conditions. The theoretical results are in good agreement with experimental measurements.

The forward saturation current density may be electron emission limited, ion emission limited, or plasma limited, depending upon the operating conditions. Furthermore, this quantity cannot exceed an absolute upper limit which depends only upon the emitter temperature and the interelectrode spacing, and is independent of the emitter work function and cesium pressure.

The forward and reverse saturation current densities and open-circuit voltage are useful in diagnostics. Under appropriately selected operating conditions, measurements of these quantities may be used to infer values of the emitter temperature, emitter work function, collector work function, electron mobility, and ion mobility.